

Michelle X. Bui, David L. Hysell
Cornell University

OBJECTIVES:

- Investigate QP echoes from sporadic-E layer observed in the upper mid-latitudes
- Determine a causal link between observations of unique sporadic-E structuring and neutral wind shear in the lower thermosphere

CORNELL RADAR:

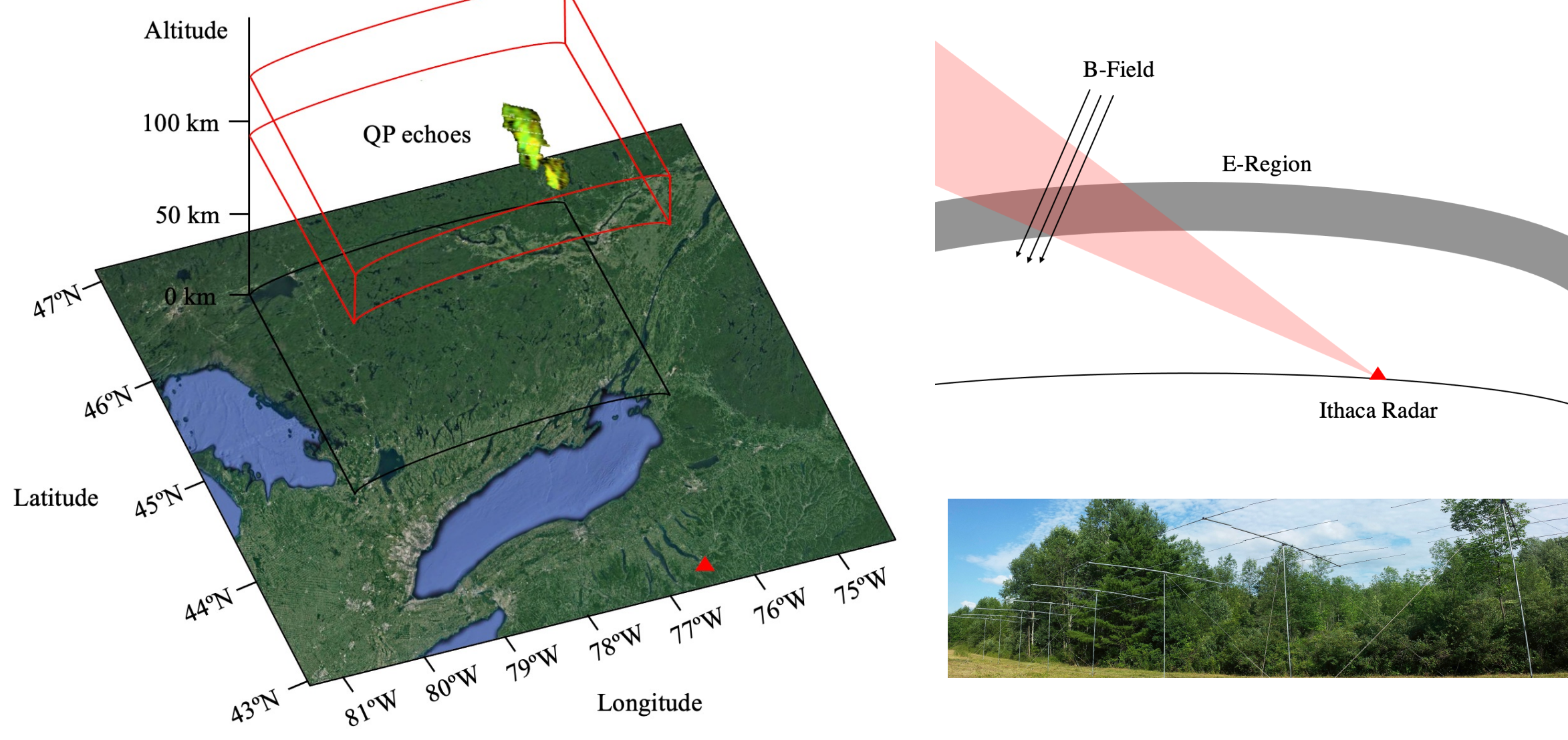


Figure 1: Schematic of Cornell radar near Ithaca, NY

BACKGROUND:

A previous study done with this radar was published by Hysell and Larsen (2021) for QP echoes captured in 2020, linking Kelvin-Helmholtz (KH) instability to backscatter observed in 2020.¹ This study focused primarily on planar wind shear and KH instability as a causal link to some of the observed structuring in sporadic-E.

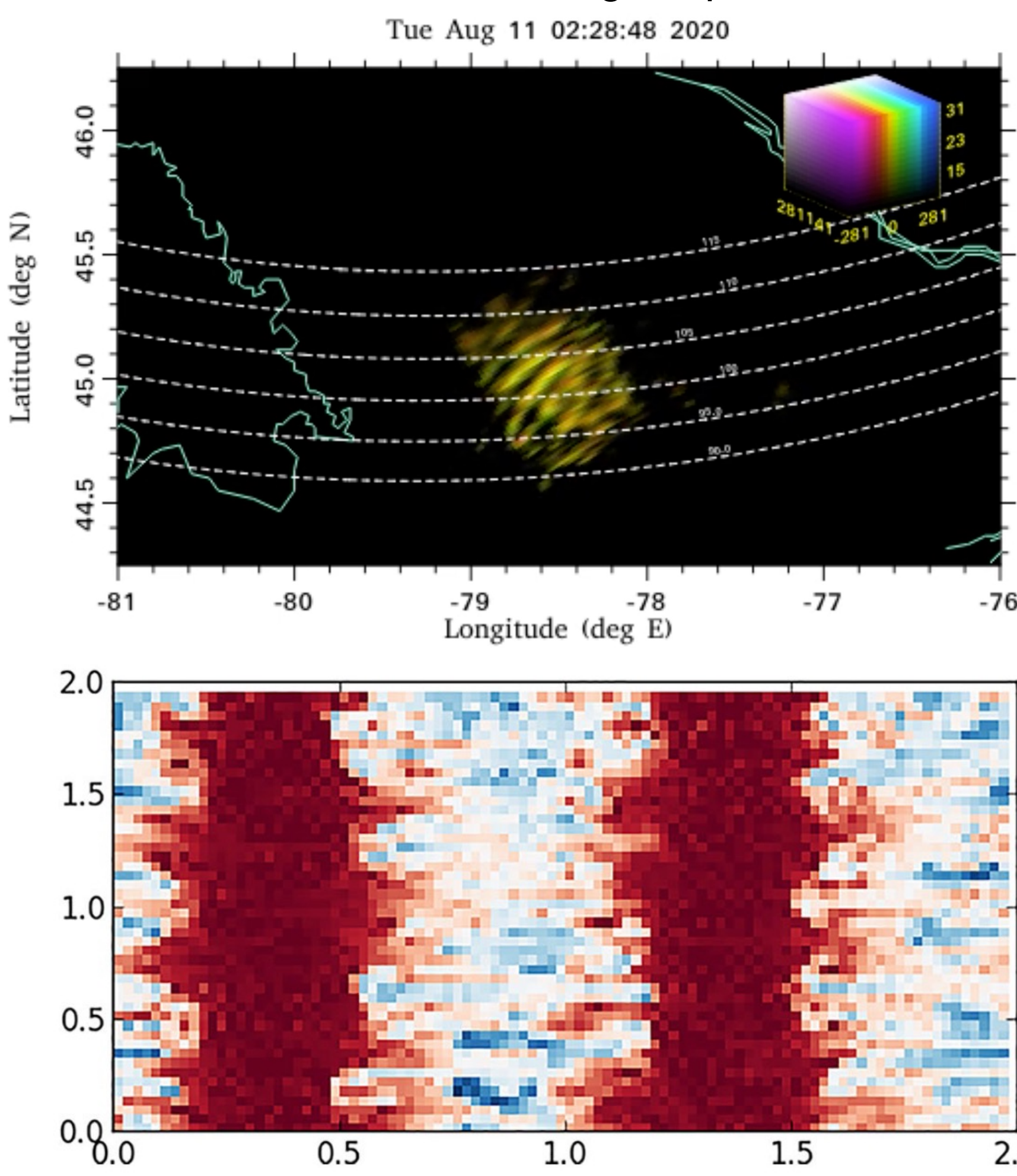


Figure 2: (a) Radar image representative of coherent backscatter received on Aug. 11, 2020 revealing fine structure in sporadic-E ionization. (b) KH simulations.¹

While KH instabilities are commonly evident in the mesosphere-lower thermosphere (MLT) region, Larsen et al. (2004) and Hurd et al. (2009) have both suggested the connection between neutral winds in the MLT region to analogous structures in the atmospheric boundary layer, which is known to exhibit many instabilities including Ekman-type spiral flows.^{2,3}

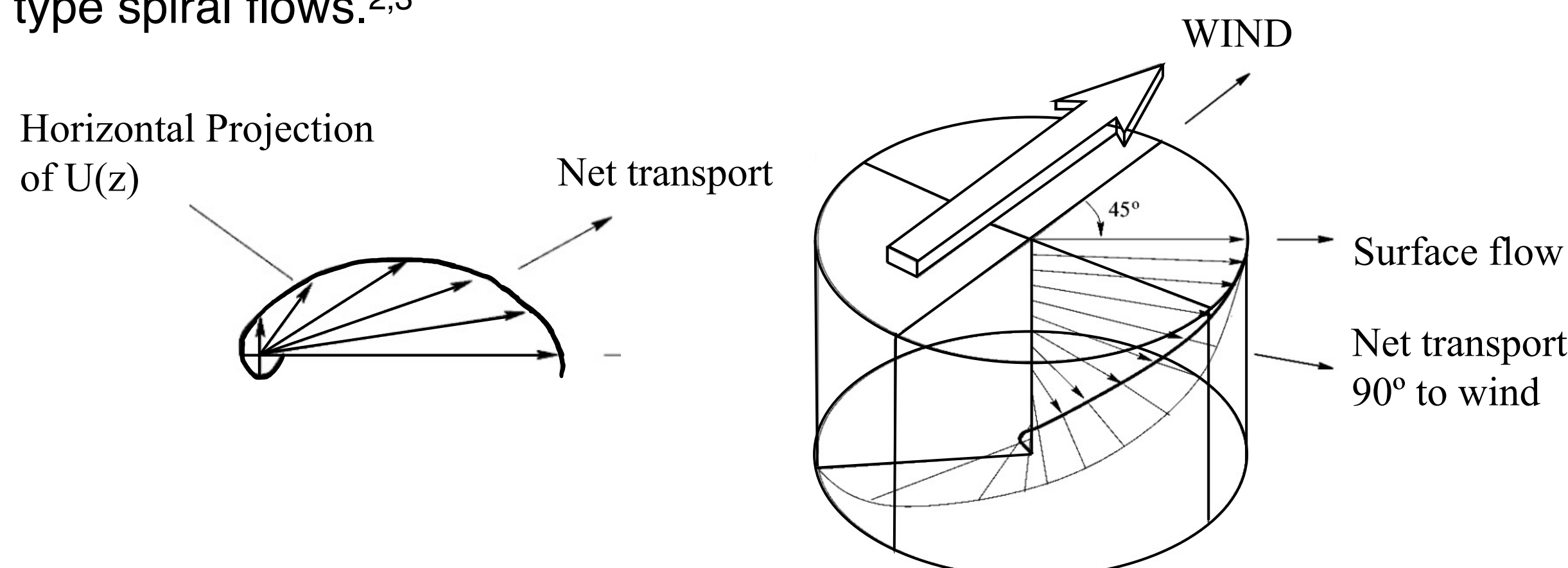


Figure 3: Schematic of Ekman spiral, illustrating geostrophic flow. Diagram from Allen and Bridges (2003).⁴

The stability of Ekman-type flows was investigated by Lilly (1966), who determined observations of a parallel wave type for Re greater than 55 and a cross-flow wave type for Re greater than 110.⁵ Further, Dubos et al. (2007) observed the emergence of secondary instabilities for Re greater than 300.⁶ Recently, Chkhetani and Shalimov (2013) have proposed a causal link between Ekman-type instabilities and frontal structures in sporadic-E instability.⁷

EXTERNAL LINKS:

To watch the [radar movie](#) or [Ekman simulation](#) in action, scan this QR code or go to the following link:
<https://linktr.ee/michellxbui>



OBSERVATIONS:

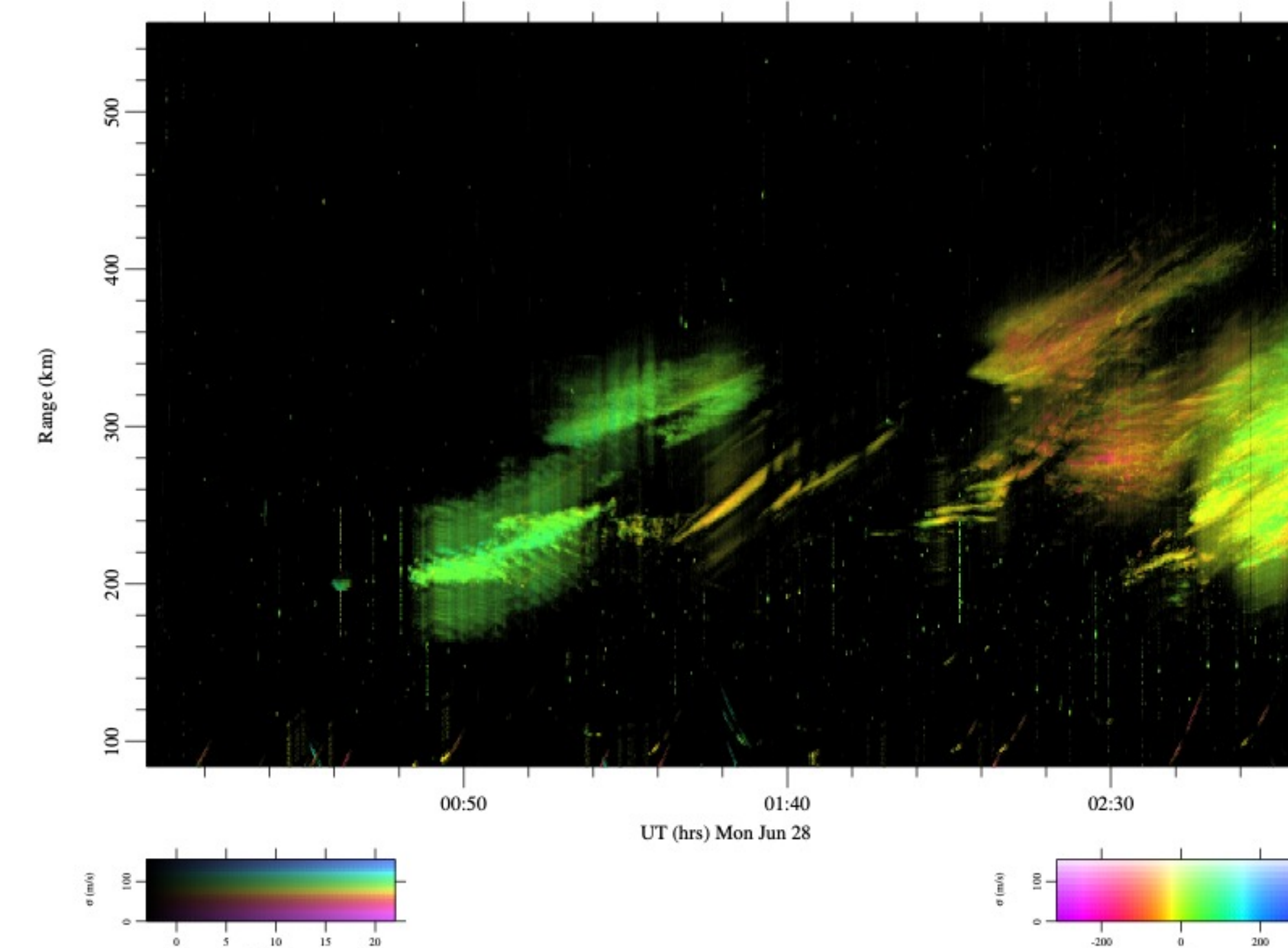


Figure 4: Range-Time-Doppler shift plot on Jun. 28, 2021 at 00:00 – 03:00 UTC. The legend below each figure correspond pixel brightness, hue, and saturation to signal-to-noise ratio, Doppler shift, and spectral width of backscatter from sporadic E layer.

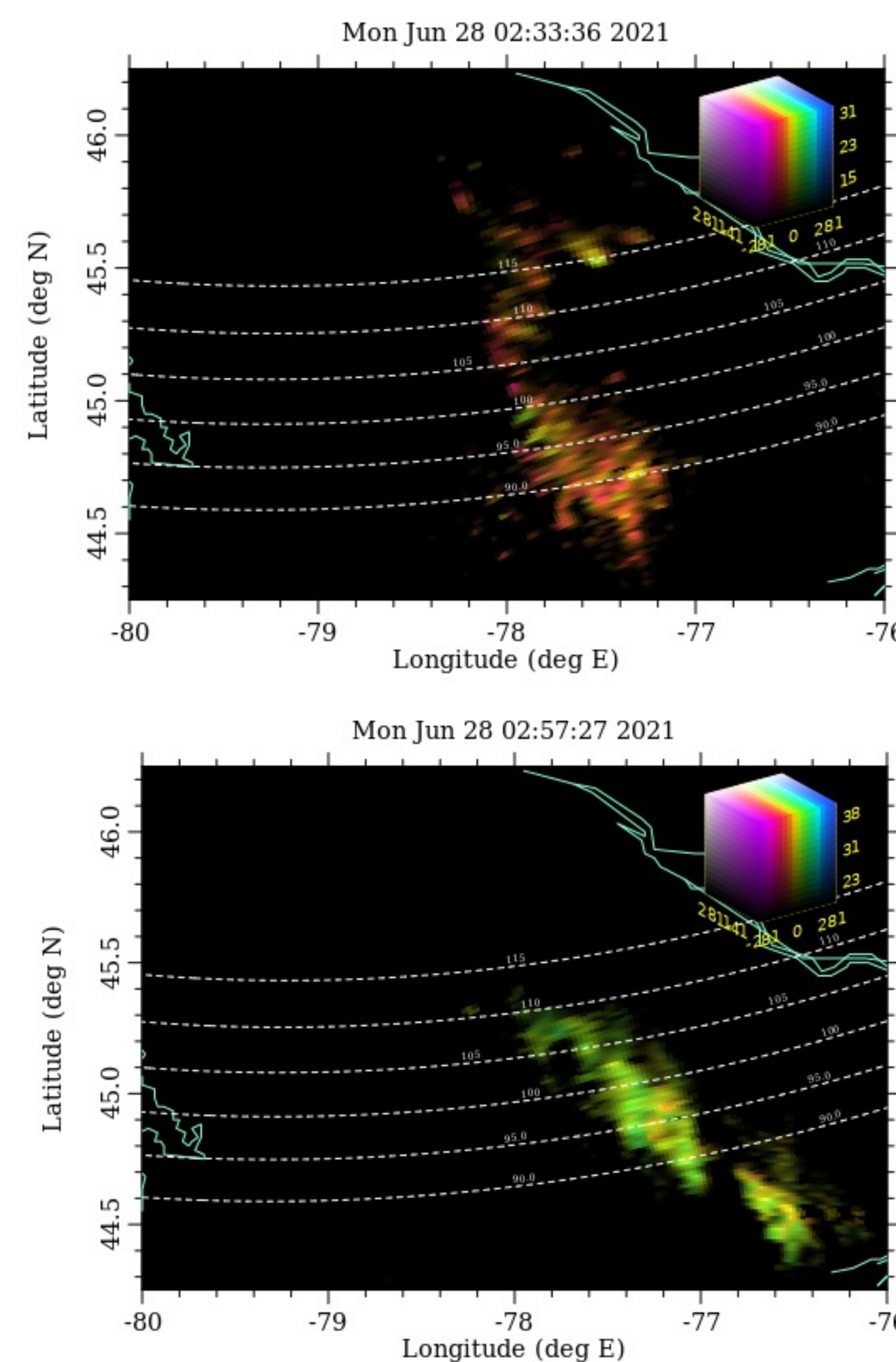


Figure 5: Radar images representative of coherent backscatter received on Jun. 28, 2021 showing (a) horizontally-banded structure with primary bands crossed by secondary bands and (b) narrow, long-banded characterized by short primary banded structure.

THEORY & EQUATIONS:

Ekman-type instabilities are an exact solution of the Navier-Stokes equation that balance the Coriolis force, pressure gradient force, and viscosity.⁴ The following equation set was used in modeling an Ekman-type flow in the neutral thermosphere, where a boundary condition is imposed for zero flow at the boundary of $z = 0$.

Equation 1 describes the continuity equation under incompressible flow.

$$\nabla \cdot \bar{u} = 0 \quad (1)$$

Equation 2 is the Navier-Stokes equation in 3D.

$$\frac{\partial \bar{u}}{\partial t} + (\bar{u} \cdot \nabla) \bar{u} = -\frac{1}{\rho} \nabla p - 2\Omega \hat{k} \times \bar{u} + \nu \nabla^2 \bar{u} \quad (2)$$

Equation 3 is the convection-diffusion equation, which is used as a passive tracer for the motion of plasma in the ionosphere.

$$\frac{\partial S}{\partial t} + \bar{u} \cdot \nabla S = D \nabla^2 S \quad (3)$$

Equations 4-8 show the functions that satisfy the Ekman system.

$$u = \cos(\alpha) - e^{-z} \cos(z - \alpha) \quad (4)$$

$$v = \sin(\alpha) + e^{-z} \sin(z - \alpha) \quad (5)$$

$$w = 0 \quad (6)$$

$$p = p_0 + 2x \sin(\alpha) - 2y \cos(\alpha) \quad (7)$$

$$S = e^{-z/\alpha} \quad (8)$$

MODELING & ANALYSIS

Figures 4(a-c) show the results of the Ekman-type instability simulation for $Re = 330$ using the Dedalus package.⁸

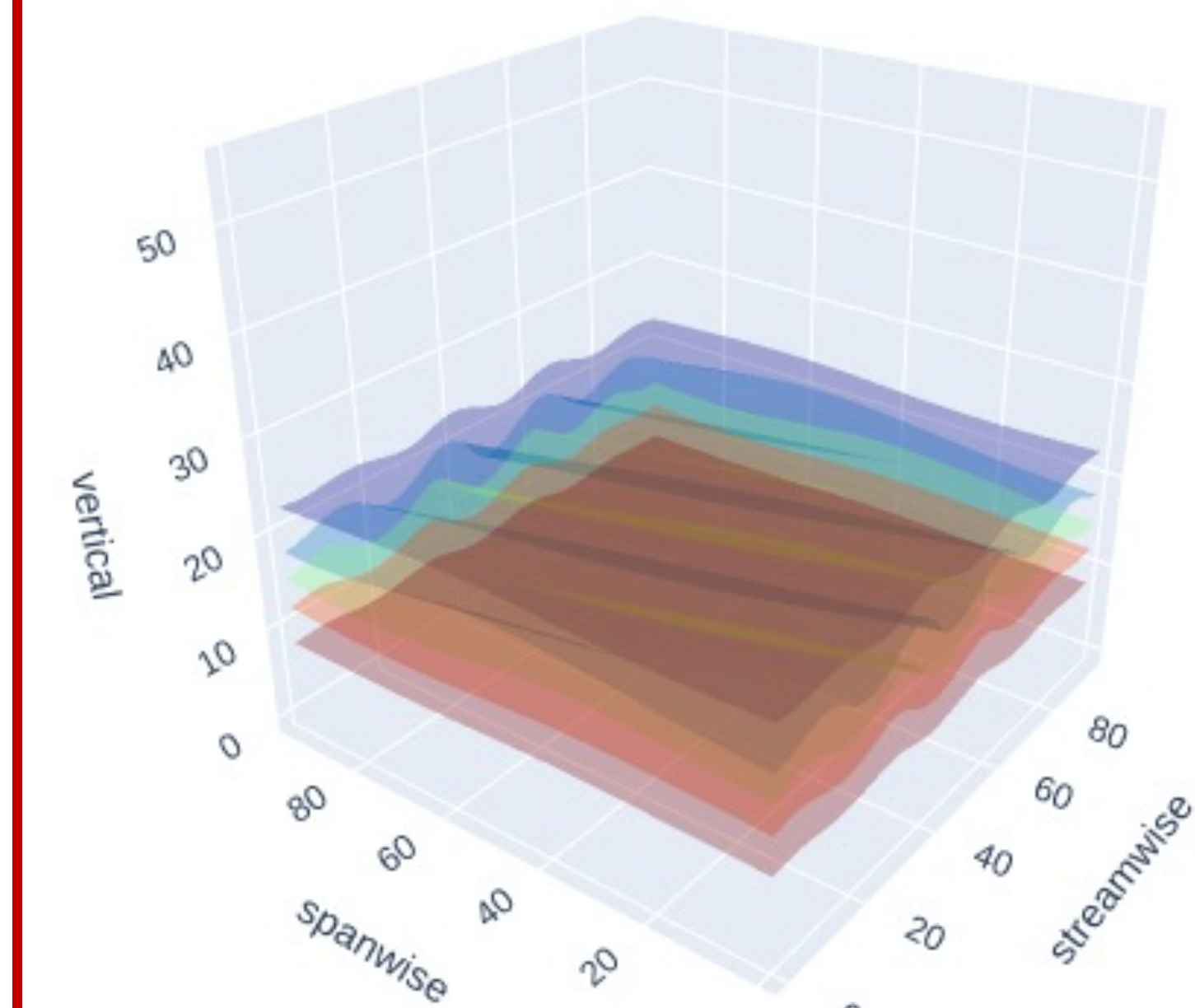


Figure 6(a): Flow after 52 min. of initialization reveals a viscous, travelling type wave evident by parallel flow.

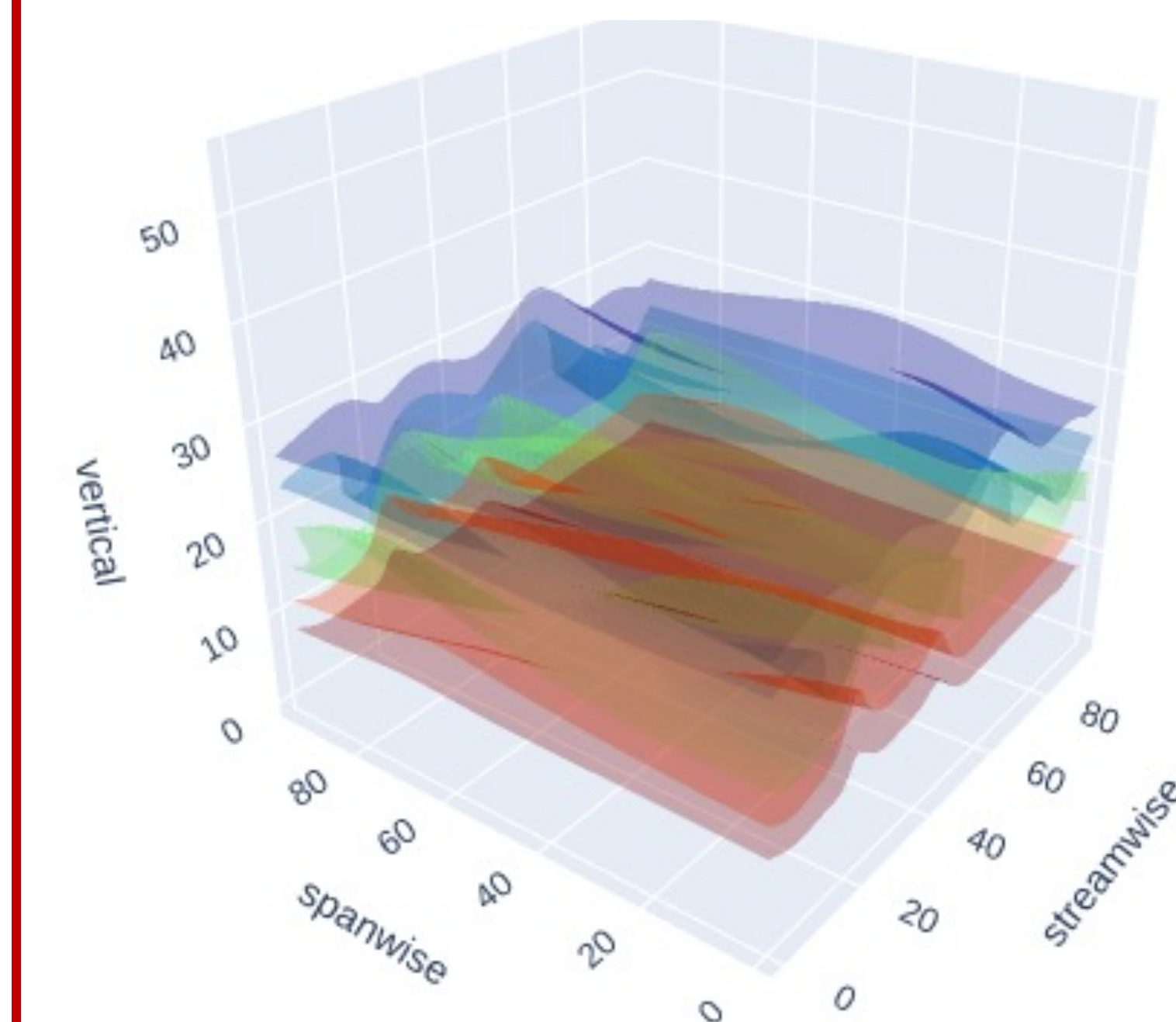


Figure 6(b): Flow after 104 min. of initialization reveals an inviscid, cross-flow type wave.

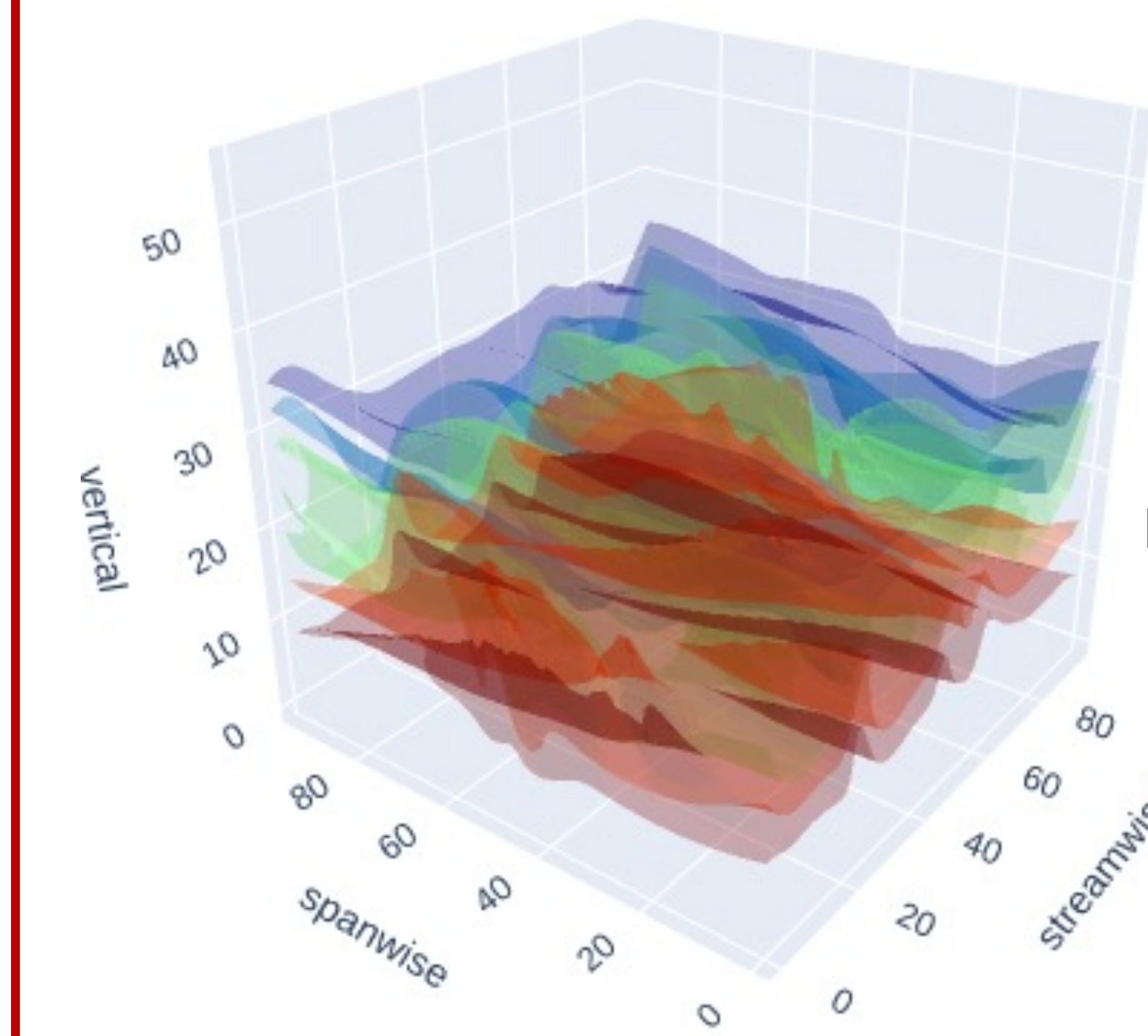


Figure 6(c): Flow after 156 min. of initialization reveals secondary wave breaking.

Simulation Parameters

| | |
|---------------------------|-------------------|
| Characteristic Length L | 1 km |
| Characteristic Velocity U | 100 m/s |
| Simulation box | 40 L x 40 L x 6 L |
| Incident angle α | 90° |

CONCLUSION:

- We propose that sporadic-E structures observed by the Ithaca radar may correspond to mixing in the MLT region, particularly Ekman-type spiral flows.
- Future direction: further computational models of MLT mixing, incorporation of plasma equations, physical investigation of MLT neutral wind structure in the upper mid-latitude region.
- This work was supported by NSF awards AGS-2011304 to Cornell University and AGS-2012994 to Clemson University.

REFERENCES:

- Hysell and Larsen. (2021) VHF imaging radar observations and theory of banded midlatitude sporadic E ionization layers. *J. Geophys. Res. Space Phys.* 126.
- Larsen et al. (2004) Observations of overturning in the upper mesosphere and lower thermosphere. *J. Geophys. Res.* 109.
- Hurd et al. (2009) Overturning instability in the mesosphere and lower thermosphere: analysis of instability conditions in lidar data. *Ann. Geophys.* 27: 2937-2945.
- Allen and Bridges. (2003) Hydodynamic stability of the Ekman boundary layer including interaction with complaint surface: a numerical framework. *Europ. J. of Mech. B/ Fluids.* 22: 239-258.
- Lilly (1966) On the Instability of Ekman Boundary Flow. *J. Atmos. Sci.* 23: 481-494
- Dubos et al. (2007) Emergence of secondary instability of Ekman layer rolls. *J. Atmos. Sci.* 65: 2326-2342.
- Chkhetani & Shalimov (2013) Mechanism by which frontal structures in the ionospheric sporadic E layers are formed. *Geomag. & Aeron.* 53(2): 177-187.
- Dedalus Project: <https://dedalus-project.readthedocs.io/en/latest/>